

Supplementary Information for

Full Pseudocapacitive Behavior Hypoxic Graphene for Ultrafast and Ultrastable Sodium Storage

Ying-Ying Wang,^{ab} Bao-Hua Hou,^d Xu Yang,^c Dong Chen,^a Hao-Jie Liang,^c Zhen-Yi Gu,^{bc} Xian-Hong Rui^{*a}, and Xing-Long Wu^{*bc}

^a Collaborative Innovation Center of Advanced Energy Materials, School of Materials and Energy, Guangdong University of Technology, Guangzhou 510006, China,
E-mail: xhrui@gdut.edu.cn.

^b Key Laboratory for UV Light-Emitting Materials and Technology of Ministry of Education, Northeast Normal University, Changchun, Jilin 130024, P. R. China,
E-mail: xinglong@nenu.edu.cn.

^c National & Local United Engineering Laboratory for Power Batteries, Faculty of Chemistry, Northeast Normal University, Changchun, Jilin 130024, P. R. China.

^d State Centre for International Cooperation on Designer Low-Carbon & Environmental Materials, School of Materials Science and Engineering, Zhengzhou University, Zhengzhou 450001, P. R. China.

* The corresponding authors, E-mail: xhrui@gdut.edu.cn; xinglong@nenu.edu.cn.

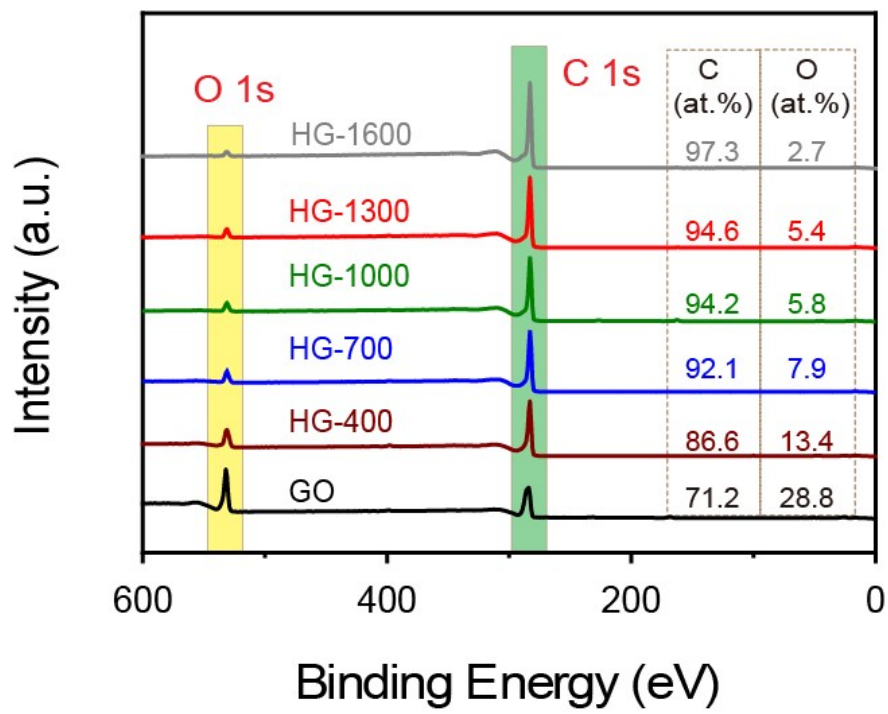


Fig. S1 The XPS spectra survey of GO, HG-400, HG-700, HG-1000, HG-1300, and HG-1600 materials.

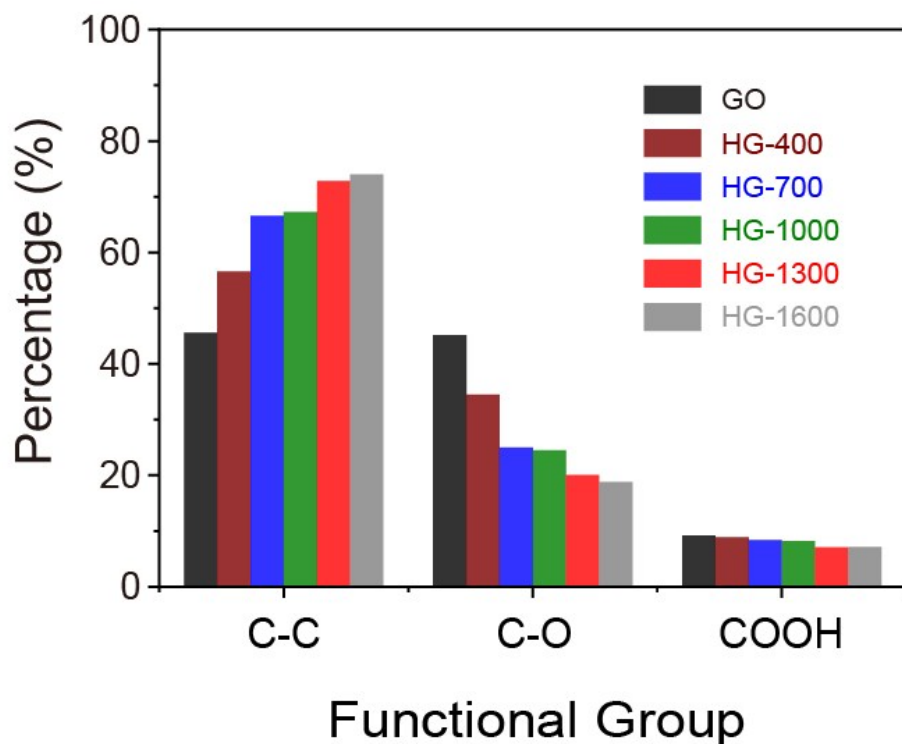


Fig. S2 The change of functional group content in materials of GO, HG-400, HG-700, HG-1000, HG-1300, and HG-1600 materials.

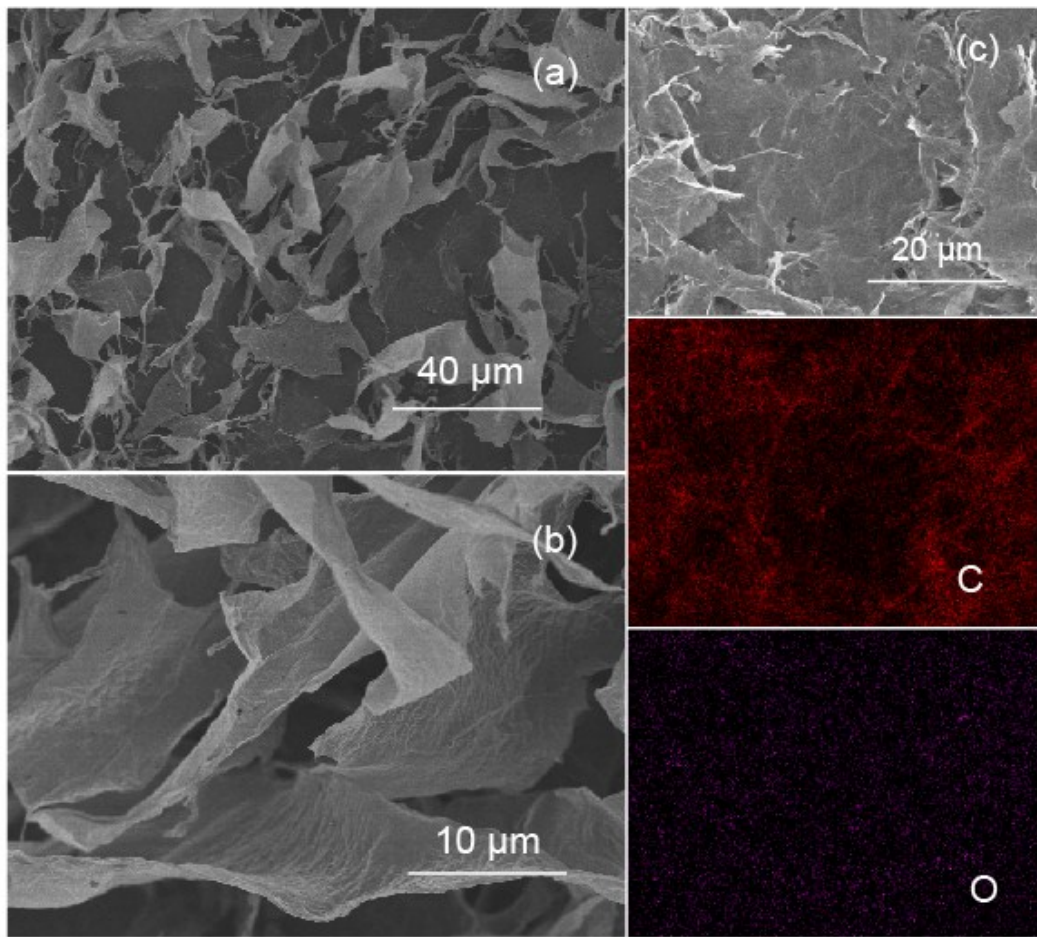


Fig. S3 (a and b) SEM images under different magnifications and (c) the elemental mapping images of the as-prepared HG-1300.

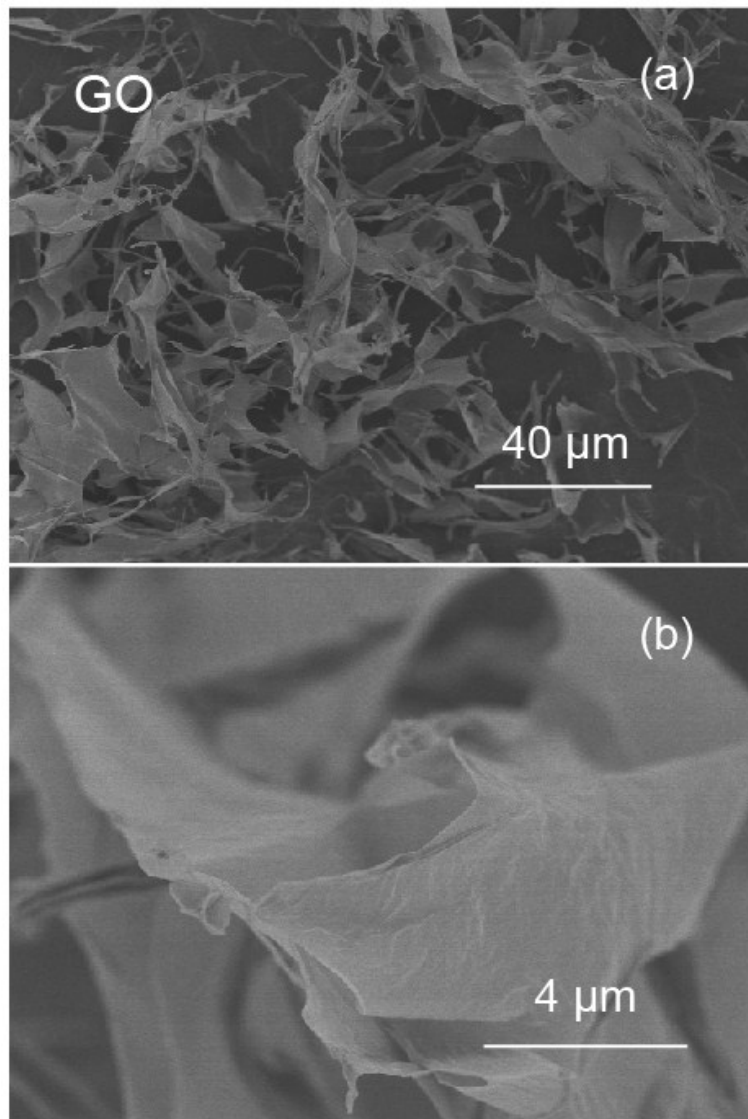


Fig. S4 (a and b) SEM images of GO under different magnifications.

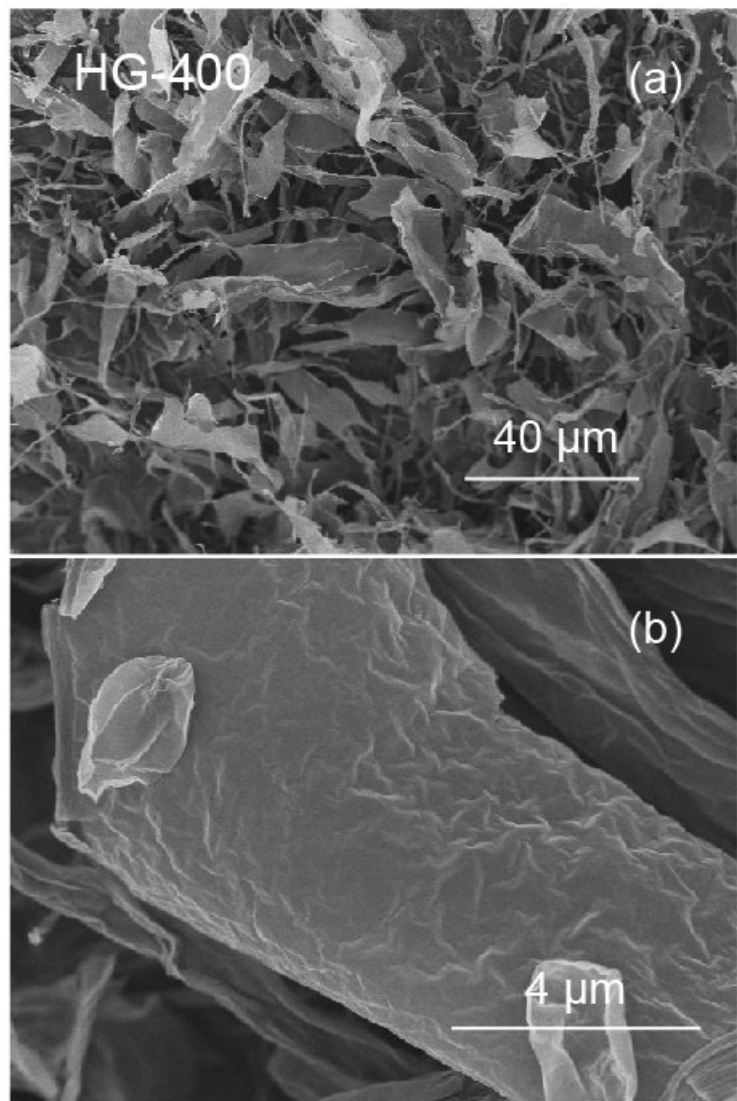


Fig. S5 (a and b) SEM images of HG-400 under different magnifications.

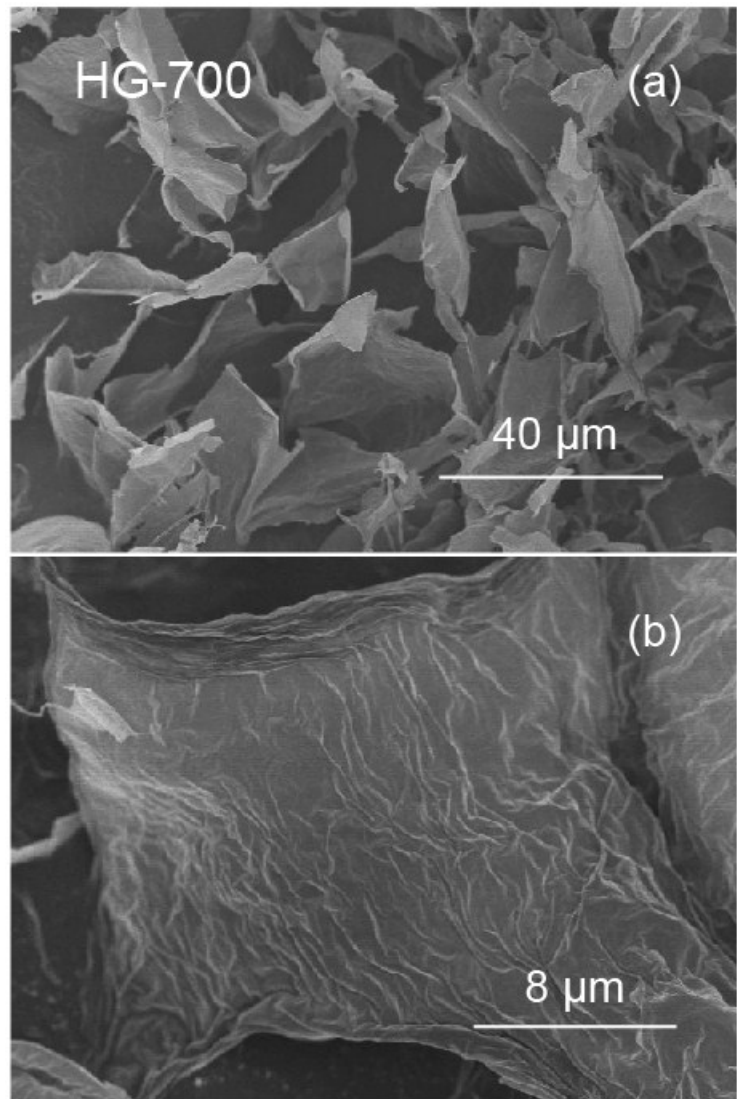


Fig. S6 (a and b) SEM images of HG-700 under different magnifications.

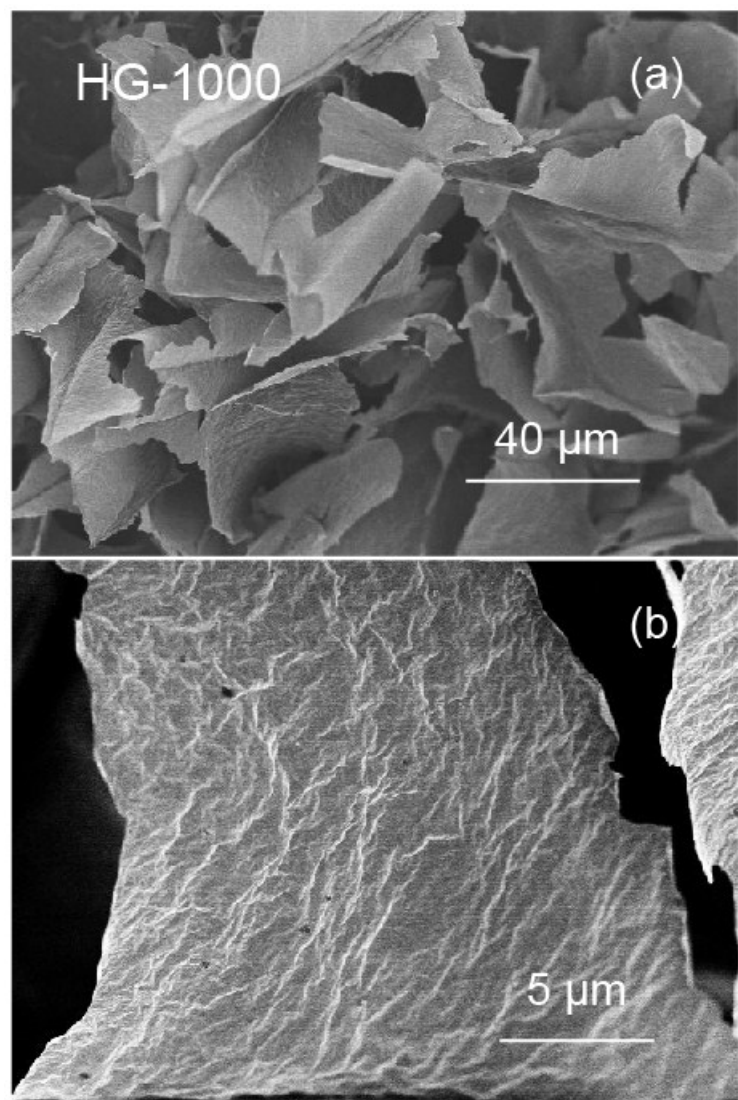


Fig. S7 (a and b) SEM images of HG-1000 under different magnifications.

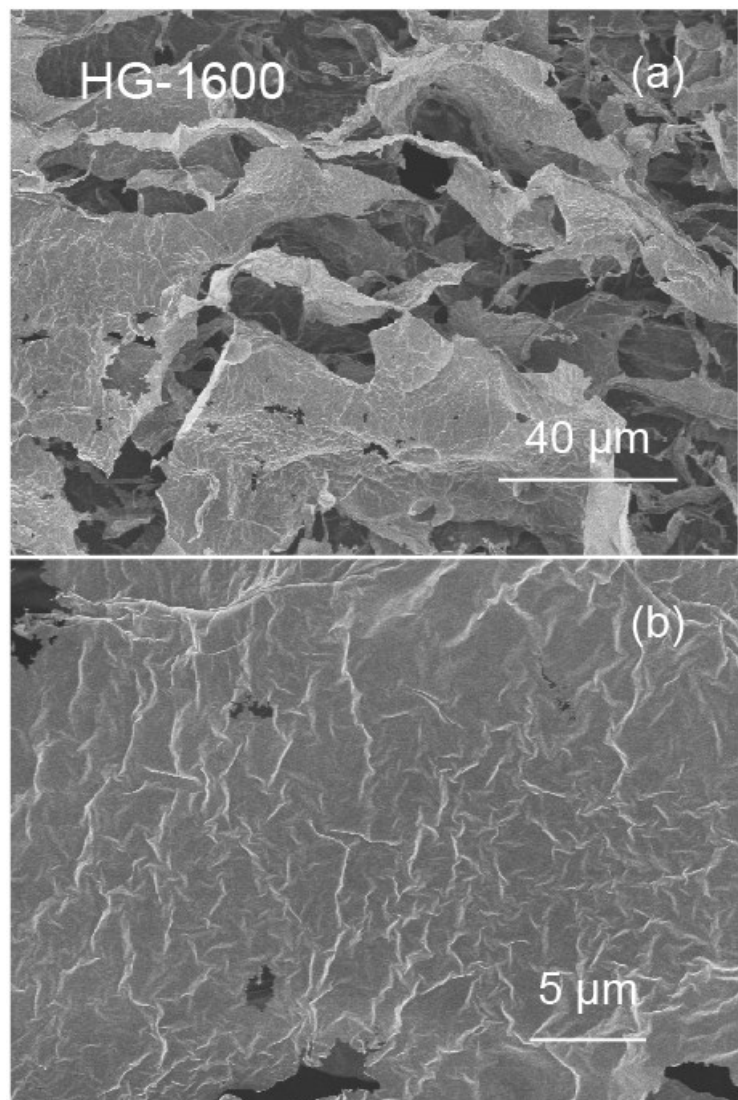


Fig. S8 (a and b) SEM images of HG-1600 under different magnifications.

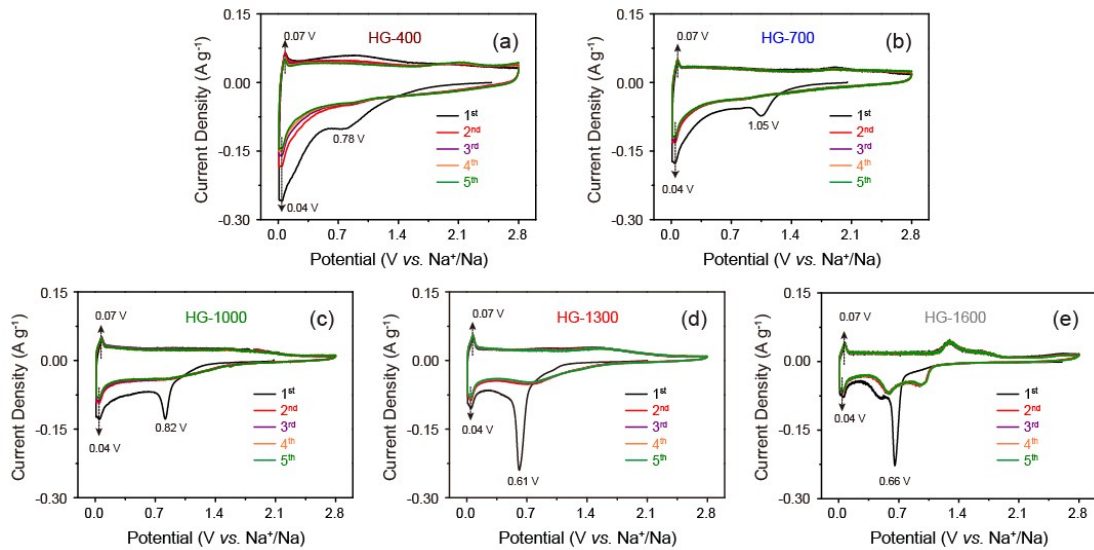


Fig. S9 CV curves of the initial 5 cycles for the HG-400, HG-700, HG-1000, HG-1300, and HG-1600 electrodes in the potential range of 0.01-2.8 V at a scan rate of 0.1 mV s^{-1} .

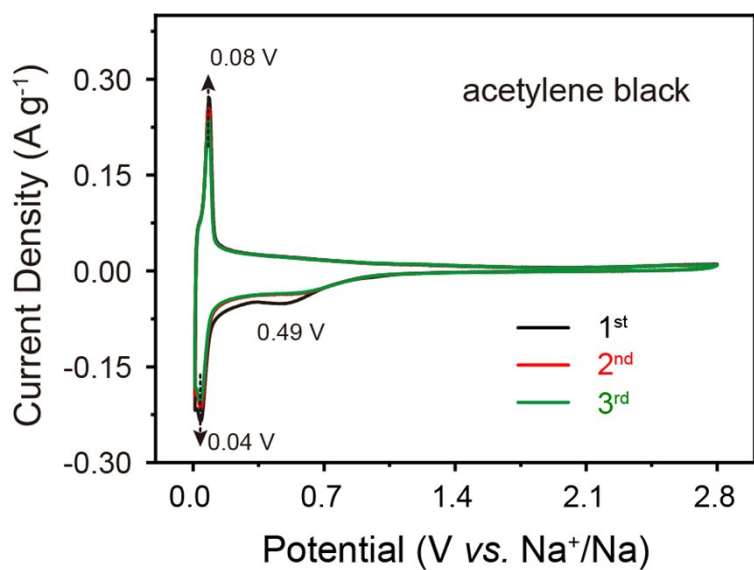


Fig. S10 CV curves of the first 3 cycles for the acetylene black.

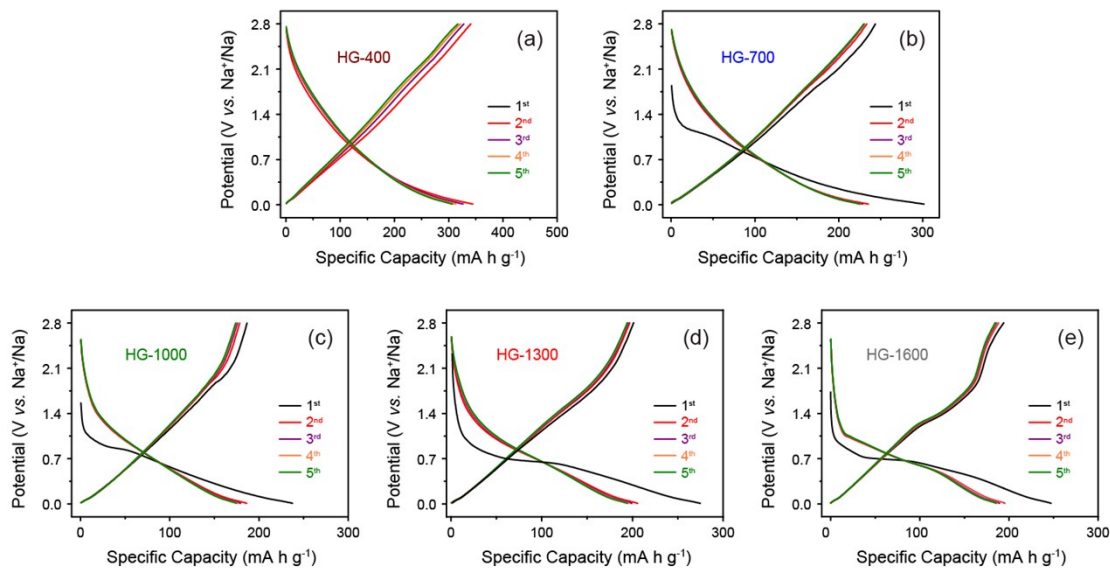


Fig. S11 Galvanostatic charge/discharge curves of the initial 5 cycles for the HG-400, HG-700, HG-1000, HG-1300, and HG-1600 electrodes in the potential range of 0.01-2.8 V at 0.05 A g⁻¹.

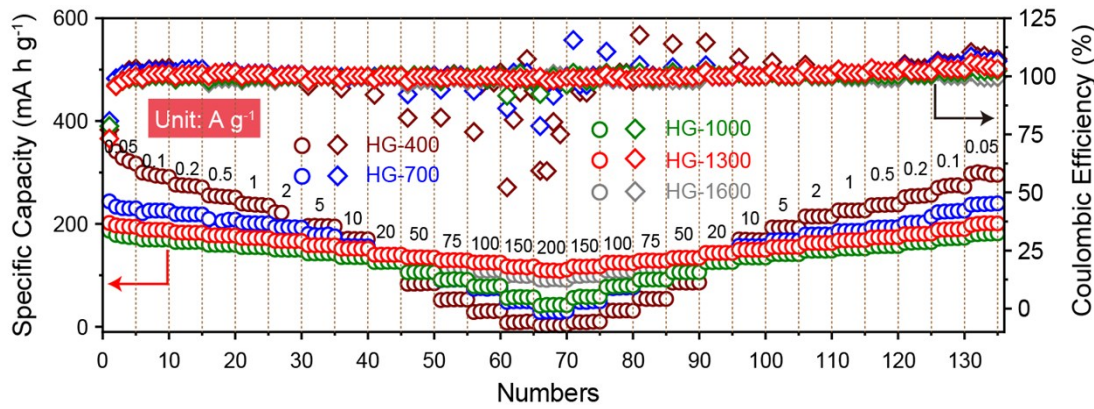


Fig. S12 Rate capability of the HG-400, HG-700, HG-1000, HG-1300, and HG-1600 electrodes at different current densities (Range: from 0.05 to 200 A g⁻¹, then return to 0.05 A g⁻¹ in turn).

As shown in Fig. S12, the initial specific capacities of HG-400, HG-700, HG-1000 and HG-1300 are 370.3 mA h g⁻¹, 243.6 mA h g⁻¹, 186.6 mA h g⁻¹ and 201.7 mA h g⁻¹, respectively. The reversible specific capacity of the HG-1300 is significantly lower than that of the HG-400 and HG-700. This is mainly due to the fact that the HG-1300 material prepared by high-temperature calcination contains a smaller amount of oxygen-containing functional groups. We know that, during charging/discharging, the oxygen-containing functional groups on graphene can store a part of sodium ions. The reaction contributes a portion of the specific capacity, but this portion of the capacity is not very stable; it will significantly diminish as the current density increases.

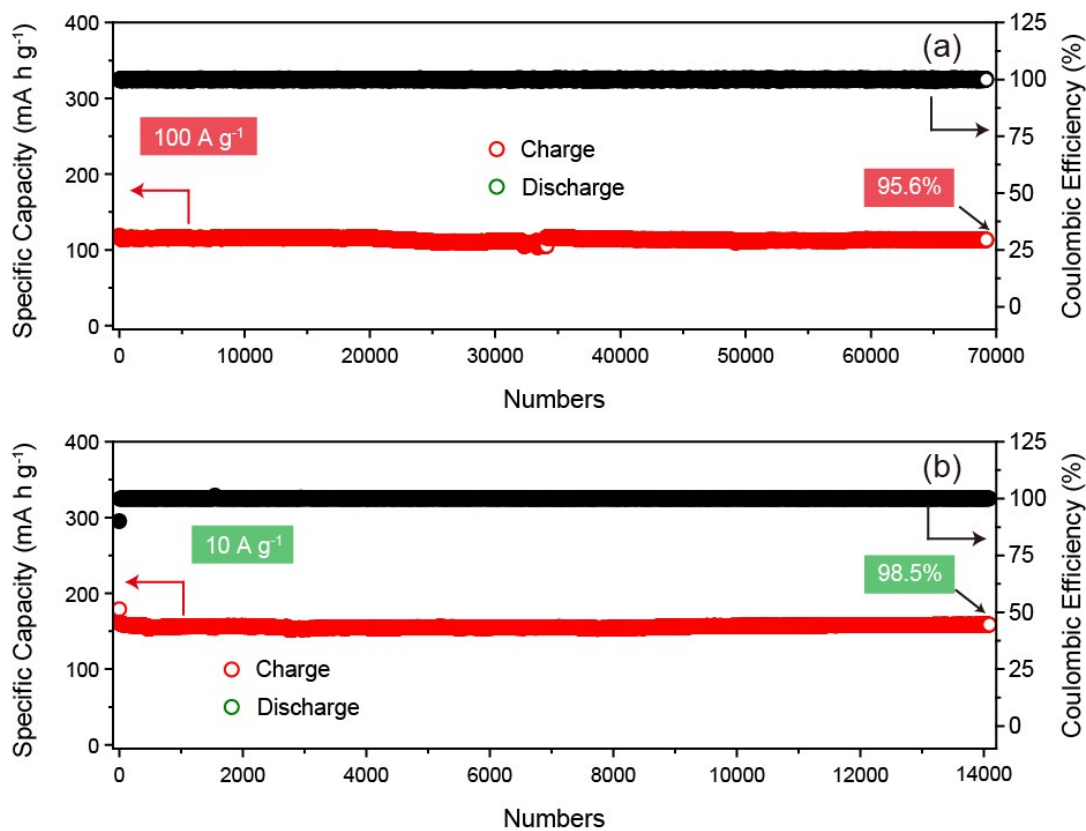


Fig. S13 Cycle performance of the HG-1300 electrode at 100 A g^{-1} and 10 A g^{-1} .

Table S1. Comparisons of cycling performances in this study with the previously reported carbon-based materials for Na storage. As shown, the present HG-1300 exhibits excellent cycle stability.

Materials	j (A g ⁻¹)	Cycles (r)	Reversible capacity (mA h g ⁻¹)	Retention (%)	Decay rate per cycle (%)
	20	100 000	121.1	90.7	0.000093
HG-1300	10	14 000	158.8	98.5	0.000107
	100	70 000	113.2	95.6	0.000063
S-MCN-700 ¹	0.1	100	304.2	35.2	0.35
HC ²	1.0	2 000	196	90	0.005
HC ³	0.2	1 500	72.3	84	0.0107
C-600 ⁴	10	15 000	115	~100	--
CPP ⁵	0.2	200	203.3	98	0.01
3D PCFs ⁶	5	10 000	99.8	95.9	0.00041
3D N-GF ⁷	0.5	150	594	69.7	0.202
S-N/C ⁸	1	1 000	211	86	0.014
FP-MP 5:2 1000 ⁹	0.15	100	191	74	0.26
N-FLG-800 ¹⁰	0.5	2 000	210	98.6	0.0007
LPHC ¹¹	1	1 000	150	85	0.015
COAT-10- 1400 ¹²	0.1	100	286	97	0.03
HCSs-CNTs ¹³	1.0	500	95.1	60	0.08
RHHC-1300 ¹⁴	0.025	100	346	93	0.07
NCL@GF ¹⁵	0.5	2 500	279	70	0.012
NC-550 ¹⁶	0.1	200	212	76.1	0.1195
NNCS ¹⁷	0.03	200	243.1	85	0.075
CF ¹⁸	0.2	200	169	97.7	0.0115
CNS ¹⁹	1	500	190	71.9	0.0562

HPNSC ²⁰	0.2	3 350	160.5	76	0.0072
without H ₃ PO ₄ treatment ²¹	0.2	220	181	84.6	0.07
AC111400 ²²	0.03	150	226	89	0.073
NMC600 ²³	0.05	300	268.9	71.46	0.095
SN-HCS ²⁴	0.5	2 000	169	81.25	0.0094
CPs ²⁵	0.02	100	298.1	99.3	0.007
LS1400 ²⁶	0.1	450	330	94	0.013
CC700 ²⁷	1	8 000	105	85	0.001875
N-HC ²⁸	5	10 000	101.4	97.3 ^{1000th}	0.0003
carbonized CNC ²⁹	0.1	400	300	88.2	0.0295
SGCN ³⁰	5	5 000	161.8	73.6	0.00528
HCP ³¹	2	1 000	176.8	75	0.025

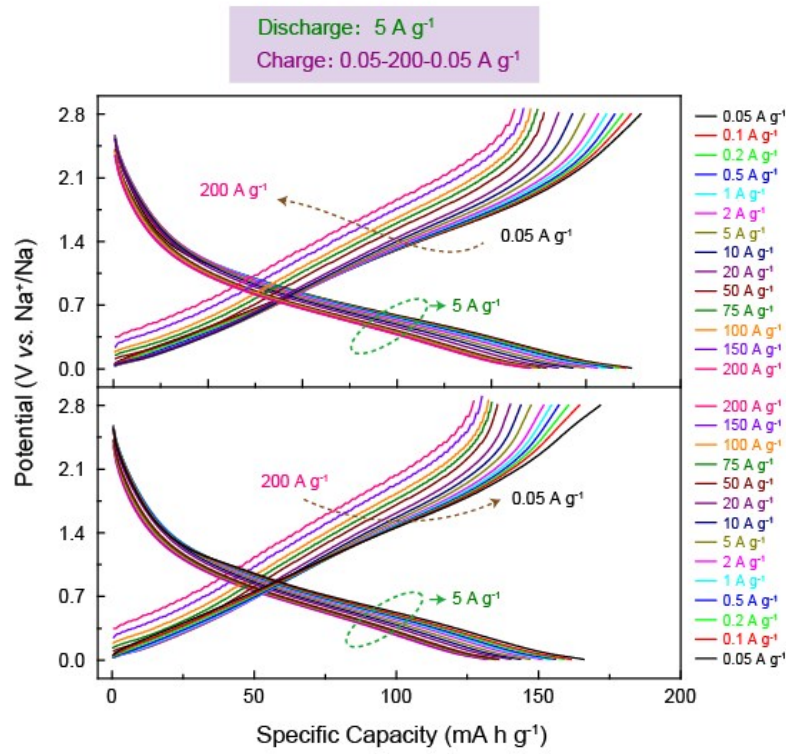


Fig. S14 Galvanostatic charge/discharge curves at different current densities.

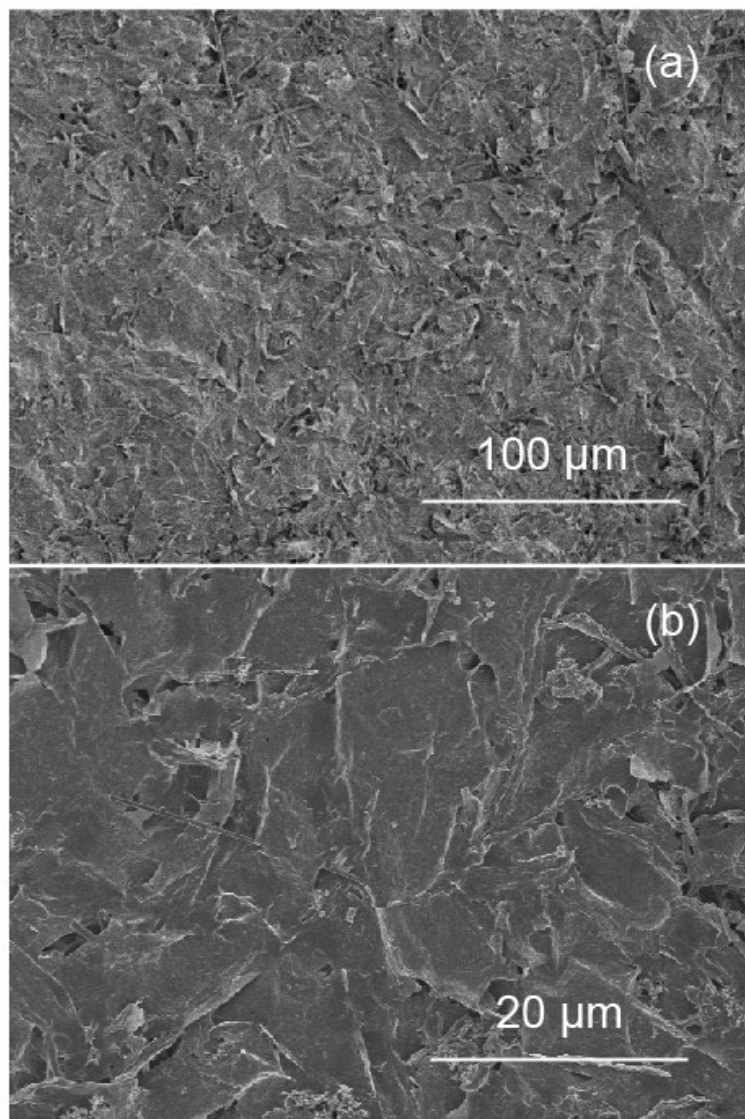


Fig. S15 (a and b) the SEM images of the HG-1300 electrode after 6000 cycles at the state of 5 A g^{-1} discharge and 1 A g^{-1} charge.

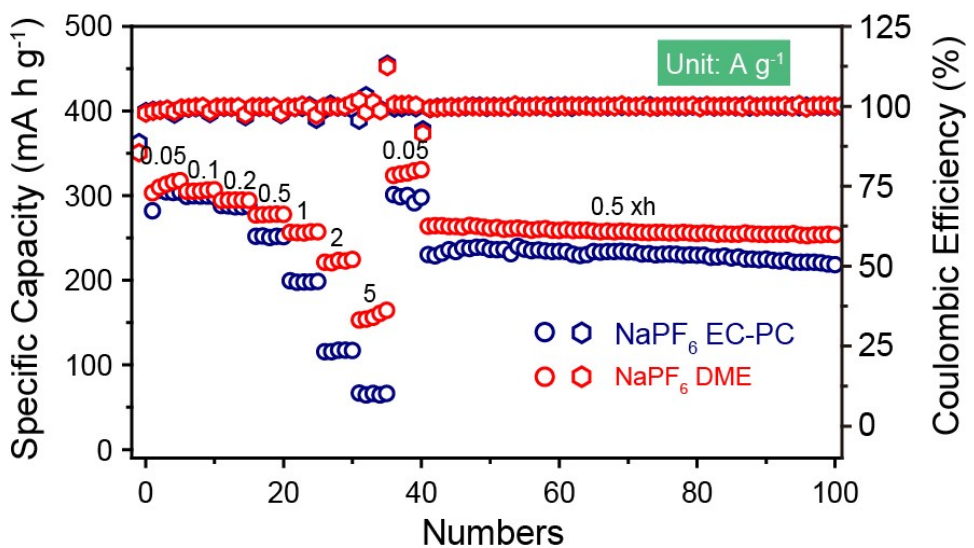


Fig. S16 Rate capability comparison for CSC electrode in 1 M NaPF_6/DME and 1 M $\text{NaPF}_6/\text{EC-PC}$ electrolytes.

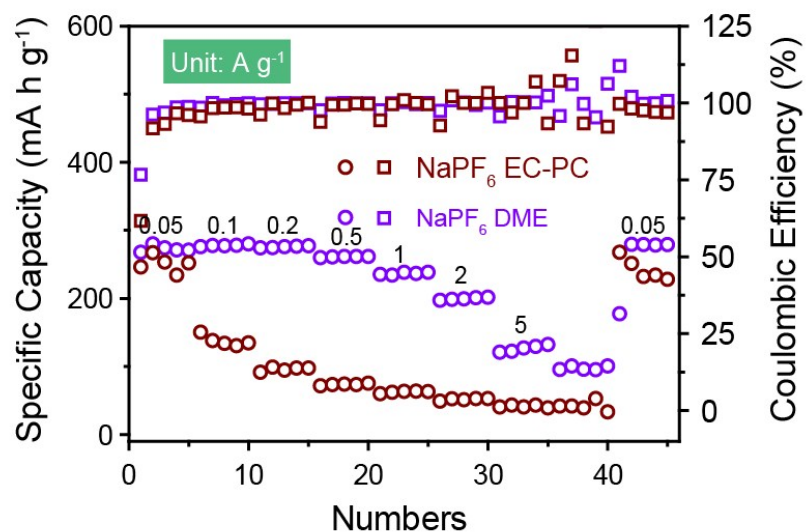


Fig. S17 Rate capability comparison for LSC electrode in 1 M NaPF₆/DME and 1 M NaPF₆/EC-PC electrolytes.

References:

1. W. Cha, I. Y. Kim, J. M. Lee, S. Kim, K. Ramadass, K. Gopalakrishnan, S. Premkumar, S. Umapathy and A. Vinu, *ACS Appl. Mater. Interfaces*, 2019, **11**, 27192-27199.
2. Y. He, P. Bai, S. Gao and Y. Xu, *ACS Appl. Mater. Interfaces*, 2018, **10**, 41380-41388.
3. X. Liu, X. Jiang, Z. Zeng, X. Ai, H. Yang, F. Zhong, Y. Xia and Y. Cao, *ACS Appl. Mater. Interfaces*, 2018, **10**, 38141-38150.
4. N. Wang, Y. Wang, X. Xu, T. Liao, Y. Du, Z. Bai and S. Dou, *ACS Appl. Mater. Interfaces*, 2018, **10**, 9353-9361.
5. Y. Zhang, X. Li, P. Dong, G. Wu, J. Xiao, X. Zeng, Y. Zhang and X. Sun, *ACS Appl. Mater. Interfaces*, 2018, **10**, 42796-42803.
6. H. Hou, C. E. Banks, M. Jing, Y. Zhang and X. Ji, *Adv. Mater.*, 2015, **27**, 7861-7866.
7. J. Xu, M. Wang, N. P. Wickramaratne, M. Jaroniec, S. Dou and L. Dai, *Adv. Mater.*, 2015, **27**, 2042-2048.
8. J. Yang, X. Zhou, D. Wu, X. Zhao and Z. Zhou, *Adv. Mater.*, 2017, **29**, 1604108.
9. F. Xie, Z. Xu, A. C. S. Jensen, H. Au, Y. X. Lu, V. Araullo-Peters, A. J. Drew, Y. S. Hu and M. M. Titirici, *Adv. Funct. Mater.*, 2019, **29**, 1901072.
10. J. Liu, Y. Zhang, L. Zhang, F. Xie, A. Vasileff and S. Z. Qiao, *Adv. Mater.*, 2019, **31**, e1901261.
11. B. Xiao, F. A. Soto, M. Gu, K. S. Han, J. Song, H. Wang, M. H. Engelhard, V. Murugesan, K. T. Mueller, D. Reed, V. L. Sprenkle, P. B. Balbuena and X. Li, *Adv. Energy Mater.*, 2018, **8**, 1801441.
12. Q. Li, Y. Zhu, P. Zhao, C. Yuan, M. Chen and C. Wang, *Carbon*, 2018, **129**, 85-94.
13. L. Suo, J. Zhu, X. Shen, Y. Wang, X. Han, Z. Chen, Y. Li, Y. Liu, D. Wang and Y. Ma, *Carbon*, 2019, **151**, 1-9.
14. Q. Wang, X. Zhu, Y. Liu, Y. Fang, X. Zhou and J. Bao, *Carbon*, 2018, **127**, 658-666.
15. B. Chang, J. Chen, M. Zhou, X. Zhang, W. Wei, B. Dai, S. Han and Y. Huang, *Chem. Asian J.*, 2018, **13**, 3859-3864.
16. C. Liu, J. Hu, L. Yang, W. Zhao, H. Li and F. Pan, *Chem. Commun.*, 2018, **54**, 2142-2145.
17. A. Agrawal, S. Janakiraman, K. Biswas, A. Venimadhav, S. K. Srivastava and S. Ghosh, *Electrochim. Acta*, 2019, **317**, 164-172.
18. T. Chen, Y. Liu, L. Pan, T. Lu, Y. Yao, Z. Sun, D. H. C. Chua and Q. Chen, *J. Mater. Chem. A*, 2014, **2**,

4117-4121.

19. Y. Chen, L. Shi, S. Guo, Q. Yuan, X. Chen, J. Zhou and H. Song, *J. Mater. Chem. A*, 2017, **5**, 19866-19874.
20. Y. Y. Wang, B. H. Hou, Q. L. Ning, W. L. Pang, X. H. Rui, M. Liu and X. L. Wu, *Nanotechnology*, 2019, **30**, 214002.
21. K.-I. Hong, L. Qie, R. Zeng, Z.-q. Yi, W. Zhang, D. Wang, W. Yin, C. Wu, Q.-j. Fan, W.-x. Zhang and Y.-h. Huang, *J. Mater. Chem. A*, 2014, **2**, 12733-12738.
22. Y. Li, Y.-S. Hu, H. Li, L. Chen and X. Huang, *J. Mater. Chem. A*, 2016, **4**, 96-104.
23. H. Liu, M. Jia, S. Yue, B. Cao, Q. Zhu, N. Sun and B. Xu, *J. Mater. Chem. A*, 2017, **5**, 9572-9579.
24. J. Ye, J. Zang, Z. Tian, M. Zheng and Q. Dong, *J. Mater. Chem. A*, 2016, **4**, 13223-13227.
25. Z. Zhu, F. Liang, Z. Zhou, X. Zeng, D. Wang, P. Dong, J. Zhao, S. Sun, Y. Zhang and X. Li, *J. Mater. Chem. A*, 2018, **6**, 1513-1522.
26. N. Zhang, Q. Liu, W. Chen, M. Wan, X. Li, L. Wang, L. Xue and W. Zhang, *J. Power Sources*, 2018, **378**, 331-337.
27. R. Hao, Y. Yang, H. Wang, B. Jia, G. Ma, D. Yu, L. Guo and S. Yang, *Nano Energy*, 2018, **45**, 220-228.
28. X. Hu, X. Sun, S. J. Yoo, B. Evanko, F. Fan, S. Cai, C. Zheng, W. Hu and G. D. Stucky, *Nano Energy*, 2019, **56**, 828-839.
29. H. Zhu, F. Shen, W. Luo, S. Zhu, M. Zhao, B. Natarajan, J. Dai, L. Zhou, X. Ji, R. S. Yassar, T. Li and L. Hu, *Nano Energy*, 2017, **33**, 37-44.
30. G. Zou, C. Wang, H. Hou, C. Wang, X. Qiu and X. Ji, *Small*, 2017, **13**, 1700762.
31. B. H. Hou, Y. Y. Wang, Q. L. Ning, W. H. Li, X. T. Xi, X. Yang, H. J. Liang, X. Feng and X. L. Wu, *Adv. Mater.*, 2019, **31**, e1903125.